Scrape off layer heat transport and divertor power deposition of pellet induced ELMs

RP Wenninger[1], TH Eich[2], GTA Huysmans[3], PT Lang[2], S Devaux[2], S Jachmich[4], F Köchl[5] and JET EFDA Contributors*

JET-EFDA, Culham Science Centre, Abingdon, OX14 3DB, UK

[1] *Universitätssternwarte der Ludwig-Maximilians-Universität, 81679 München, Germany*

[2] *Max-Planck-Institut für Plasmaphysik, EURATOM Association, Garching, Germany*

[3] *ITER Organization, Bat 519, CEA Cadarache, 13108 St. Paul-lez-Durance, France*

[4] *Laboratory for Plasma Physics, Ecole Royal Militaire/Koninklijke Militaire School, B-1000 Brussels, Belgium*

[5] *Association EURATOM-ÖAW, Atominstitut, TU Wien, 1020 Wien, Austria*

* *See the Appendix of F. Romanelli et al., Proceedings of the 23rd IAEA Fusion Energy Conference 2010, Daejeon, Korea*

Introduction

It is currently assumed that a reliable control technique for ELMs is mandatory for the success of ITER to meet restrictions in power loads to the target [1, 2, 3]. In view of next step fusion devices it is of paramount importance to reach some level of understanding in the process of inducing ELMs by pellets. Due to the technically given toroidal asymmetric nature of pellet injection the question arises, if the spatial structure of the perturbation associated with pellet induced ELMs features a corresponding toroidal asymmetry in the SOL and in the divertor. The paper recapitulates the finding of a toroidal asymmetric divertor deposition pattern during pellet induced ELMs employing a new JET divertor infrared system and compares these to nonlinear simulations.

Experimental observations

Divertor infrared tomography (IR) in combination with magnetic field line tracing has previously been employed to investigate the structure of spontaneous ELMs [3]. We apply this method in conjunction with a ramp of the toroidal magnetic field (2.2T to 2.8T, q_{95} 4.8 to 3.6) in order to manipulate the position of the divertor imprint of a (transient) toroidally localised filament. Some key parameters of the discharge analyzed in this paper (79573) are: $I_P = 2.0MA$, $P_{NBI} \approx 8MW$ and $\delta = 0.27$ (low triangularity). Figure 1a displays the evolution of a number of further parameters. Pellets of a nominal particle content of 2×10^{21} ($\sim 30\times$trigger threshold [4]) have been injected perpendicularly from the magnetic low field side mid plane at 4Hz with velocities between 170m/s and 200m/s.

As already shown in [5] significant differences according to the divertor deposition structure have been observed during spontaneous and pellet induced ELMs. Figure 1b shows the radial target position of the largest peaks of the divertor power flux density profiles defined by a threshold criterion versus $|B_T|$. The threshold criterion is fulfilled when the local power flux density exceeds 85% of the maximum power flux density within the profile during an investigated period (t=0 to t=0.4ms with t=0 defined by the peak power deposition). One can see that the locations of most peaks associated with pellet induced ELMs show a clear correlation with $|B_T|$, while spontaneous ELMs have peaks scattering arround the same location for all values of $|B_T|$.

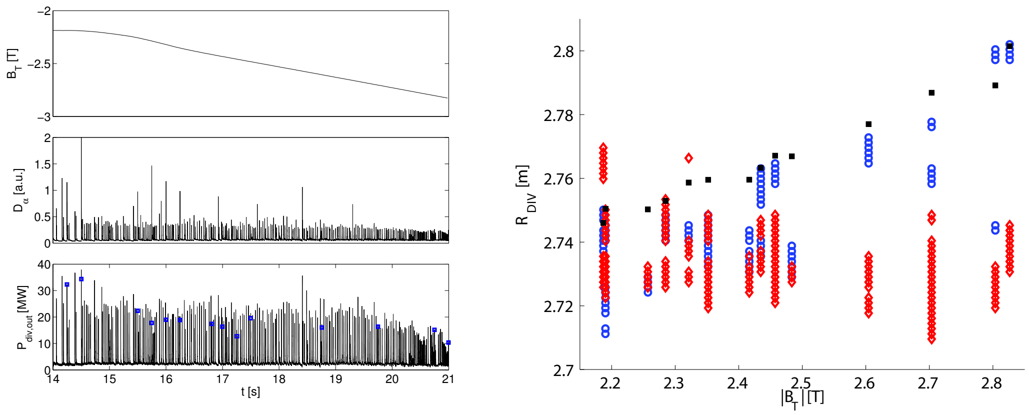

Figure 1: a) Time traces of toroidal magnetic field, D_α-radiation, power to the outer target, edge line integrated density and pellet monitor signal. b) Observed peak positions (criterion is described in the text) for pellet induced ELMs (blue dots) and spontaneous ELMs (red dots) as function of $|B_T|$ in discharge 79573 (Fueling size pellets / LFS): Squares indicate predicted and corrected peak positions on the basis of field line tracing with $\Phi_{mp} = \Phi_{pel}$.

A comparative analysis of various divertor power load aspects has been carried out [5, 6]. Here spontaneous and pellet induced ELMs chosen on the basis of selection criteria described in [6] have been analyzed. A maximum power flux density on the outer target during the entire ELM of $23 \pm 5\,\mathrm{MW/m^2}$ for spontaneous and $30 \pm 7\,\mathrm{MW/m^2}$ for pellet induced ELMs has been found.

Code predictions from JOREK

The non-linear MHD code JOREK [7] evolves a set of reduced MHD equations in 3D.The computational domain includes the plasma center, the separatrix, the x-point and the open field lines in the SOL. For the simulation of pellet induced ELMs a JET-like H-mode plasma [8] has been chosen with an pedestal pressure gradient such that the plasma is marginally stable with respect to low to medium-n ballooning modes. In the simulations the pellet is described by a large local particle source located in the middle of the pedestal at the magnetic low field side with a half-width of 2 cm and acting adiabatically on the plasma.

Figure 2a) shows a contour of the density as well as the temperature on the separatrix and the heat flux convected to the target $\sim 50\mu s$ after the start of the pellet source. A helical perturbation with the dominant toroidal mode number n=1 can be observed. At this time the pressure in the pellet cloud at the mid plane is about twice the pressure at the top of the pedestal and remains relatively constant. Figure 2b) shows a close-up of the density profile at the toroidal angle where the pellet cloud is passing the x-point. Here as well the contours of the electrostatic potential (ExB flow lines) from the JOREK calculation are illustrated. From the high density region of the helical pellet cloud there is an ExB flow across the separatrix close to the x-point directed towards the divertor. This ExB flow is found by the model to be clearly stronger towards the outer divertor leg, which is the one with the higher simulated power flux densities on the divertor.

The ExB flow leads to prompt losses of particles close to the x-point. Since the particles crossing the separatrix have been heated by parallel transport inside the separatrix, we expect that

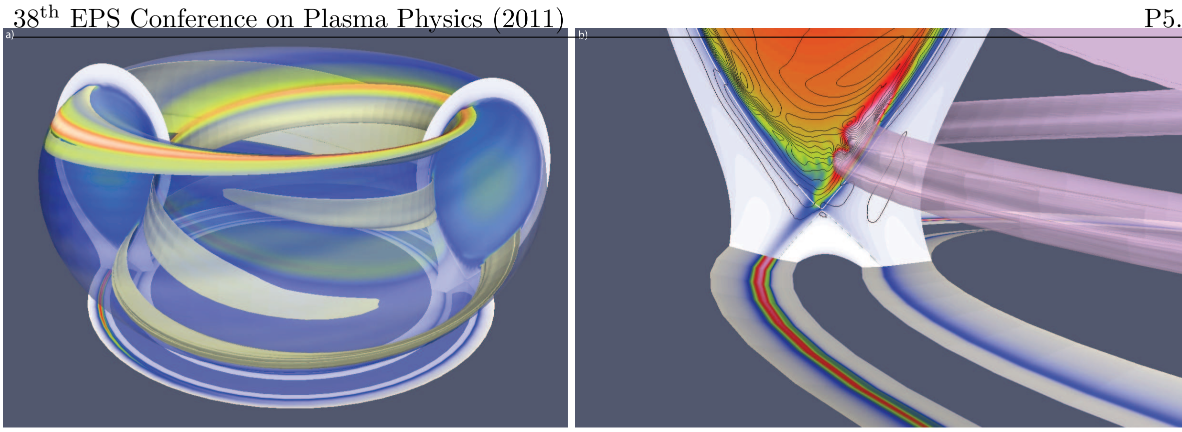

Figure 2: a) The density contour ($n = 1.1 \times n_{mag.axis}$) at $t \sim 50\mu s$, the temperature at the separatrix (red-blue scale) and the convected heat flux to the target. The pellet injection location is on the LFS mid plane on the side of the plasma, which is turned away from the viewer. b) Close-up of the density contour together with the contours of the electrostatic potential (ExB flow lines, black contours). The heat convected to the target is illustrated in both figures.

there is also an associated convected heat transport. After the separatrix crossing the parallel transport might have a more dominant role.

Figure 3a) illustrates the power flux density on the outer divertor calculated by JOREK for a time $\sim 40\mu s$ after the onset of the particle source as a function of radial divertor position R_{div} and toroidal angle Φ. At a radial position of 3.25m there is high or even maximum deposition for all toroidal angles. This position corresponds to the separatrix mapped on the outer divertor target. In addition to this symmetric deposition component another component changing maximum power flux density and profile shape with the toroidal angle can be observed. This component is spreading toroidally towards a symmetric shape with approximately the local sound speed in the x-point region.

In order to isolate the asymmetric component we identify the toroidal angle, for which the power flux density integrated along the radial direction is minimum (fig. 3c). We select the radial power flux density profile for this toroidal angle as the profile, which describes in the best way the symmetric component. We subtract this profile of the power flux density profiles for each toroidal angle and obtain the profiles of the asymmetric component, which are shown in figure 3b). Figure 3d) illustrates the profiles for the toroidal position with the maximum asymmetric contribution.

The maximum power flux density of the total deposition evaluated for each toroidal position has a maximum variation of 66% of the mean value, which is a much larger variation then the experiment describes. Thus a considerable toroidal asymmetry in the maximum power flux density is predicted by JOREK. Figure 3d) indicates the location of the maximum power flux density for all toroidal locations for the total deposition and the asymmetric component. In real space coordinates the line for the total deposition would appear as a structure similar to a spiral.

By means of JOREK calculations and SOL field line tracing a number of indications regarding the nature of the toroidally asymmetric component of the transport associated with pellet induced ELMs has been gathered. As further discussed in [5] there are two candidate positions for the separatrix crossing: a) X-point region and b) pellet injection location.

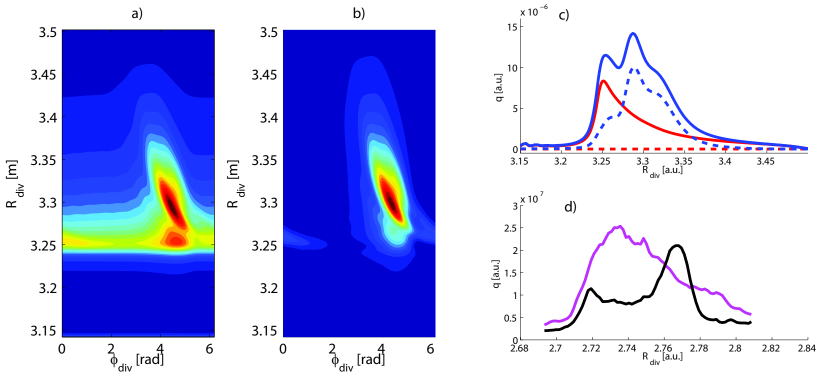

Figure 3: Heat flux density on the outer divertor target from JOREK simulation: a) Total deposition b) Asymmetric component. Pellet injection location is at $\Phi = 0$. c) Profiles of total deposition (solid) and asymmetric component (dashed) at toroidal position with minimum (red) and maximum (blue) asymmetric contribution. d) Deposition profile of individual ELMs averaged over t=0 to to t=0.4ms with t=0 defined by the peak power deposition: Pellet induced ELM (black) and spontaneous predecessor (magenta)

Summary

We recall that the ultimate goal of inducing ELMs by pellets is the reduction of the deteriorating effect of the ELMs on the plasma facing components [9]. In the light of this the striking feature of pellet induced ELMs to cause an asymmetric divertor power load deserves particular attention. In the simulation the toroidal variation of the maximum power flux density is 66% for the total deposition. In qualitative comparison the experiment with asymmetric component in the IR-view the peak heat flux of pellet induced ELMs is found to be considerably larger than for spontaneous ELMs. It is not clear, if the asymmetric component is of similar extent for ELMs induced by pellets injected from the high field side, or ELMs induced by smaller pellets and how it scales with major radius. Consequently it can not be excluded that pellet injection at fixed q_{95} in next step fusion devices such as ITER causes considerable toroidaly localised enhanced divertor degradation.

This work was supported by EURATOM and carried out within the framework of the European Fusion Development Agreement. The views and opinions expressed herein do not necessarily reflect those of the European Commission.

References

[1] Federici G et al 2003, J.Nucl.Mater. **313-316** 11-22
[2] Loarte A et al 2003, J.Nucl.Mater. **313-316** 962-966
[3] Eich T et al 2005, J.Nucl.Mater. **337-339** 669-676
[4] Lang P et al 2011, Nuclear Fusion **51** 1-16
[5] Wenninger R P at al 2010, 37th EPS Conf. on Controlled Fusion and Plasma Physics
[6] Wenninger R P at al 2011, Submitted to Plasma Phys. Control. Fusion
[7] Huysmans G T A et al 2009, Plasma Phys. Control. Fusion **51** 124012
[8] Huysmans G T A et al 2010, 37th EPS Conf. on Controlled Fusion and Plasma Physics
[9] Lang P et al 2004, Nuclear Fusion **44** 665-677